Dyslipidemia, metabolism and autophagy : antigen-independent modulation of T cells in atherosclerosis

Amersfoort, J.

CHAPTER 4

Modulation of lipid metabolism during dyslipidemia primes naïve T cells and affects their effector phenotype

Manuscript in preparation

J. Amersfoort[1]
H. Douna[1]
F.H. Schaftenaar[1]
L. Tambyrajah[1]
M. Ollé-Hurtado[1]
P.J. van Santbrink[1]
G.H.M. van Puijvelde[1]
S. Wink[2]
S.E. Le Dévédec[2]
I. Bot[1]
J. Kuiper[1]

[1]Division of BioTherapeutics, LACDR, Leiden University, Leiden, The Netherlands
[2]Division of Drug Discovery and Safety, LACDR, Leiden University, Leiden, The Netherlands

ABSTRACT

Lipid metabolism is a determining factor during the proliferation and differentiation of $CD4^+$ naïve T (Tn) cells into T helper and regulatory T (Treg) cells. An integral process in lipid metabolism during lipid overload is lipophagy, which is a specialized form of autophagy in which lipid droplets are targeted for lysosomal degradation. It is unclear whether dyslipidemia and modulation of lipid metabolism or lipophagy induce intrinsic changes in $CD4^+$ Tn cells which affect their effector phenotype.

Diet-induced dyslipidemia and dyslipidemia-like conditions, as mimicked by culturing $CD4^+$ Tn cells in the presence of excess lipoproteins or serum, induced liver-X-receptor (LXR) activation. Priming of $CD4^+$ Tn cells with atherogenic lipoproteins increased their proliferative capacity only in response to suboptimal antibody-induced stimulation but not antigen-induced stimulation. In line, priming of $CD4^+$ Tn cells under dyslipidemia-like conditions with serum from WTD-fed mice did not affect their proliferation in response to antigen stimulation. Interestingly, pharmacological LXR activation using T0901317 during priming inhibited the proliferation of $CD4^+$ T cells and induced Treg cell differentiation only after priming in dyslipidemia-like conditions. In line, modulation of lipid metabolism using the lysosomal inhibitor chloroquine during priming of $CD4^+$ Tn cells under dyslipidemia-like conditions decreased proliferation and decreased T helper 1 cell differentiation. *In vivo*, diet-induced dyslipidemia was not associated with increased autophagy in $CD4^+$ T cells. Interestingly, treatment of mice with chloroquine, which inhibits endolysosomal processing of lipoproteins as well as lipophagy, induced Treg cell differentiation but also increased $CD4^+$ T cell proliferation in mice with diet-induced dyslipidemia but not normolipidemia.

Altogether, modulation of lipid metabolism by LXR activation or lysosomal inhibition during the priming of $CD4^+$ Tn cells under dyslipidemia-like conditions affects the effector phenotype.

KEYWORDS

Naïve T cell, priming, lipids, LXR, autophagy, chloroquine

INTRODUCTION

A major risk factor for atherosclerosis is dyslipidemia in the form of hypercholesterolemia, as this is characterized by increased amounts of atherogenonic lipoproteins, such as low density lipoprotein (LDL). Native and modified LDL contain epitopes in its core-protein ApoB-100 which act as antigens for $CD4^+$ T cells inside atherosclerotic lesions [1,2] and accordingly promote atherosclerosis [3]. After activation by antigen-presenting cells (APC), $CD4^+$ naïve T (Tn) cells undergo a phase of cell blast, cell division and differentiation into a T helper cell subset. Cell blast and division require a distinct metabolic program to meet the biosynthetic demand which facilitates the generation of daughter cells from a single T cell clone [4]. Cell membranes consist, in part, of a phospholipid bilayer and free cholesterol molecules. Hence, lipid synthesis is among the first proteomic clusters to be upregulated upon activation of Tn cells [5], which is regulated by liver-X-receptor (LXR) [6] and sterol-regulatory element binding protein (SREBP) [7]. Activated LXR modulates cholesterol metabolism through its target genes, such as the cholesterol-efflux transporters ATP binding cassette A1 (ABCA1), which essentially promotes cholesterol efflux [8]. Hence, LXRβ-deficient T cells are hyperproliferative and pharmacological LXR activation inhibits T cell proliferation [6]. In line, T cells deficient for ABCG1, another cholesterol efflux transporter which regulates intracellular cholesterol trafficking and presumably localizes to the cell membrane [9], accumulate cholesterol and are hyperproliferative [10]. ABCG1 deficiency has also been shown to promote regulatory T (Treg) cell differentiation from naïve T cells [11]. Thus, cholesterol metabolism in T cells is a determining factor in the proliferative capacity and differentiation skewing of activated $CD4^+$ T cells.

In atherosclerosis, T helper (Th)1 cells are the main subset of $CD4^+$ T cells found in atherosclerotic lesions [12–14]. Th1 cells are characterized by high expression of the transcription factor T-bet and the secretion of interferon-gamma (IFNγ) via which Th1 cells drive atherosclerosis [15]. Another type of $CD4^+$ T cells, the Treg cell, is actually specialized in immunosuppression, through cell-cell interactions and the secretion of anti-inflammatory cytokines such as interleukin-10 (IL-10), and inhibit atherosclerosis [16]. Thus, hypercholesterolemia (or dyslipidemia) elevates the amount of antigen inside atherosclerotic lesions for T cells to respond to and cholesterol metabolism is an important factor in the inflammatory potency of T cells.

Interestingly, hypercholesterolemia has been suggested to modulate the inflammatory potency of T cells in an antigen-independent manner as well. For example, the supplementation of culture medium with cholesterol increases the proliferative capacity of wild-type T cells [10]. The majority of a cell's free cholesterol is located in the cell membrane where it modulates membrane rigidity [17,18] and lipid raft formation [19]. $CD8^+$ T cells deficient in acetyl-CoA acetyltransferase 1, the rate-limiting enzyme for cholesterol esterification, have elevated levels of free cholesterol and a more rigid cell membrane

which results in a more stable immunological synapse, enhanced T cell receptor (TCR)-signaling and increased T cell proliferation and inflammatory cytokine secretion [20]. Furthermore, lipid loaded $CD4^+$ T cells which are activated *in vitro* via antibody-mediated TCR stimulation are prone towards Th1 differentiation [21]. Additionally, as compared to $CD4^+$ T cells from normolipidemic mice, $CD4^+$ T cells from *Ldlr*$^{-/-}$ mice with diet-induced hypercholesterolemia contain different lipids and have an altered membrane lipid composition, which is associated with a more rigid cell membrane and increased T cell proliferation *in vivo* [22].

An essential organelle in the endolysosomal uptake of lipoproteins and degradation of intracellular lipid droplets is the lysosome [23]. Lysosomes contain lysosomal acid lipases (LAL), which degrade the triglycerides and cholesteryl from lipoproteins and deposit their content, being free fatty acids and cholesterol, into the cytoplasm. Autophagy is a cellular process in which intracellular cargo is targeted for lysosomal degradation through the selective or nonselective isolation of organelles by autophagosomes [24]. Lipophagy is a specific form of autophagy in which lysosomes degrade lipid droplets (LD) which have been targeted for lysosomal degradation by autophagosomal isolation membranes. In foam cells, atherogenic lipoprotein-induced LD accumulation is decreased by lipophagy-mediated LD degradation which enhances cholesterol efflux to Apo-A1 [25]. Most reports describe antigen-independent effects of dyslipidemia on T cells in the effector phase or the total $CD4^+$ T cell population. Presumably, dyslipidemia also modulates Tn cells which could affect their effector phenotype after TCR-stimulation. We define this as 'priming' of Tn cells as lipid accumulation could induce phenotypic changes in Tn cells prior to activation, which could affect the effector phenotype, as the strength of TCR-signaling and the induction of specific transcriptional programs, which drive lipid synthesis, could be altered. Through this mechanism, dyslipidemia primes Tn cells to have an altered inflammatory phenotype in their effector phase. We postulate here that lysosomal lipid handling and LXR-mediated cholesterol metabolism are an integral part of the priming effect of dyslipidemia on naïve T cells.

MATERIALS AND METHODS

Mice

All animal work was performed according to the guidelines of the European Parliament Directive 2010/63EU and the experimental work was approved by the Animal Ethics committee of Leiden University. LDL receptor deficient (*Ldlr*$^{-/-}$) mice were purchased from the Jackson Laboratory and further bred in the Gorlaeus Laboratory in Leiden, The Netherlands. Diet-induced dyslipidemia was established by feeding mice from 9-12 weeks of age a Western-type diet (WTD) containing 0.25% cholesterol and 15% cocoa

butter (Special Diet Services) for 2, 4, 8 or 16 weeks. At sacrifice, the mice were sedated and their blood was collected via orbital blood collection. Subsequently, their vascular system was perfused with PBS at a continuous low flow via heart puncture in the left ventricle after which the spleens were collected. For studies examining antibody-induced stimulation of T cells, male *Ldlr*$^{-/-}$ mice were used. For studies using antigen-induced T cell stimulation, we used male transgenic OT-II mice, purchased from the Jackson Laboratory and further bred in-house. OT-II mice have T cells which have a TCR recognizing chicken ovalbumin 323-339 peptide in the context of major histocompatibility complex II molecules. The animals were kept under standard laboratory conditions and were fed a normal chow diet (NCD) and water ad libitum.

Chloroquine treatment in vivo

The effect of chloroquine treatment on CD4$^+$ T cells was studied by feeding *Ldlr*$^{-/-}$ mice from 9-12 weeks of age an NCD or a WTD for 4 weeks. In the last three days of the experiment, mice from both diet groups were split into two groups which received a daily injection of either PBS or chloroquine (60 mg/kg) via intraperitoneal injection. After three days of chloroquine treatment, the mice were sacrificed as described above. Spleens were harvested, mashed through a 70 µm cell strainer to generate a single-cell suspension and used for CD4$^+$ T cell isolation.

Flow cytometry

Spleens were isolated and mashed through a 70 µm cell strainer. Erythrocytes were subsequently eliminated from the spleen by incubating the cells with ACK erythrocyte lysis buffer to generate a single-cell suspension prior to staining of surface markers. For analysis of surface markers, cells were stained at 4°C for 30 min. in PBS with 2% (vol/vol) fetal bovine serum (FBS). Intracellular transcription factors were stained for by following the FoxP3 staining protocol (eBioscience). All antibodies used for staining of surface markers or transcription factors were from eBioscience, BD Biosciences or BioLegend (table 1). For staining of LD using Bodipy™ 493/503 (Invitrogen), cells were stained with 1,3µg/mL Bodipy in pre-warmed PBS at room temperature for 10 minutes. Proliferation was assessed by flow cytometry by measuring the dye dilution in stimulated CD4$^+$ T cells which were labeled with 5 µM CellTrace™ Violet (Invitrogen) as per manufacturer's instructions. Flow cytometry analysis was performed on a FACSCantoII (BD Biosciences) or a Cytoflex S (Beckman Coulter) and data was analyzed using Flowjo software (TreeStar).

Cell culture

CD4$^+$ T cells or CD4$^+$CD62L$^+$CD44$^-$ naïve T (Tn) cells were isolated from spleens and peripheral lymph nodes (inguinal and mesenteric) from *Ldlr*$^{-/-}$ mice using MACS microbeads (Miltenyi Biotec). T cells were cultured in RPMI-1640 medium supplemented with

2 mM L-glutamine, 100U/mL pen/strep and 10% FBS (all from Lonza). Lipid loading of Tn cells was established *in vitro* by supplementing the medium with 5% serum from NCD- or WTD-fed mice for 48h. Alternatively, lipid loading was achieved by the addition of lipoproteins (10 µg/mL oxLDL and 50 µg/mL very low density lipoprotein (VLDL)) which were isolated from human serum through KBr density gradient ultracentrifugation as described below. Antibody-induced activation after lipid loading in Tn cells was performed using plate-bound anti-CD3e (1µg/mL; Ebioscience), anti-CD28 (1 µg/mL; Ebioscience) and 100U/mL recombinant murine IL-2 (Peprotech). The LXR agonist T0901317 (Sigma) was dissolved in dimethylsulfoxide and used at 5µM. The LXR antagonist GSK2033 (GlaxoSmith Klein) was used at 5µM. The lysosome inhibitor chloroquine diphosphate (ThermoFisher) was used at 50 µM.

OVA323 induced proliferation

Bone-marrow derived dendritic cells (BMDCs) were generated and cultured as described before [26] with the exception that 8% FCS was used. 24 hours before $CD4^+$ Tn cells were added to the BMDCs, the BMDCs were incubated with different concentrations of OVA323 peptide (Genscript) and 20 ng/mL granulocyte-macrophage colony-stimulating factor (GM-CSF) (Peprotech). Tn cells were isolated from male OT-II mice and primed with WTD-serum with or without T0901317 for 48 hours. After 48 hours, Tn cells were washed twice and added to GM-CSF-stimulated BMDCs to induce antigen-specific proliferation.

RNA and immunoblot analysis

mRNA was extracted from freshly isolated $CD4^+$ cells using the guanidium isothiocyanate (GTC) method after which cDNA was generated using RevertAid M-MuLV reverse transcriptase per manufacturer's instructions (Thermo Scientific). Quantitative gene expression analysis was performed using Power SYBR Green Master Mix on a 7500 Fast Real-Time PCR system (Applied Biosystems). Gene expression was normalized to 2-3 housekeeping genes (table 2). For immunoblot analysis, whole-cell lysates were prepared using radioimmunoprecipitation assay buffer (Cell Signaling Technology) supplemented with protease inhibitor (Roche). Protein lysates were resolved on a 15% SDS-PAGE gel and transferred to a polyvinylidene difluoride (PVDF) membrane with 0.2 µm pore-size. The membranes were probed with anti-LC3B or anti-β-actin antibodies (both from Novus Biologicals) and the proteins were detected using chemiluminescence.

Lipoprotein isolation and modification

The lipoproteins very-low density lipoprotein VLDL and LDL were isolated from non-fasted human serum using KBr-density gradient ultracentrifugation as described previously [27]. Oxidized LDL (oxLDL) was generated through copper oxidation by incubating LDL with $CuSO_4$ overnight at 37°C.

LC3 immunofluorescence

Isolated $CD4^+$ T cells were fixed with 3.7% formaldehyde in PBS and adhered to Superfrost adhesion slides (Thermo Scientific). Subsequently, the cells were permeabilized for 15 minutes at RT using 0.2% Triton-X, washed and then incubated with blocking solution containing 2% BSA and 0.2% Tween-20. Thereafter, LC3B was visualized by incubating the cells with a rabbit-anti-LC3B antibody (Thermo Scientific) and subsequently with a goat anti-rabbit Alexa Fluor 647 secondary antibody. Finally, the slides were mounted with Fluoroshield containing DAPI (Sigma). Images were taken on a confocal microscope Nikon Eclipse Ti with a 60x oil objective. The number of cells containing LC3B, were quantified manually and plotted relative to the total number of cells.

Automated segmentation of lipid droplet-lysosome colocalization

$CD4^+$ Tn cells were incubated with 50 µM chloroquine-diphosphate for 2 hours prior to the addition of 5% serum from NCD- or WTD-fed *Ldlr*$^{-/-}$ mice. The cells were incubated with serum and or chloroquine for 24 hours. After 24 hours, lipid droplets were stained using Bodipy as described above. Subsequently, the cells were stained with 60 nM Lysotracker Red DND-99 in complete RPMI-1640 medium for 30 min. at 37 °C. Hereafter, the cells were washed with PBS and stained with live-Hoechst (Sigma) for 45 min. at room temperature. Subsequently, the cells were washed and seeded on a plate coated with 5mg/mL poly-D-lysine (Sigma). Bodipy, lysotracker and Hoechst staining as well as transmitted light were monitored using a Nikon Eclipse Ti2 C2+ confocal laser microscope (lasers 540, 488 and 408 nm), equipped with a 20X (NA 0.75) , an automated stage and perfect focus system at 37 °C with humidified atmosphere and 5% CO2/air mixture from Okolab. Image preprocessing was performed in ImageJ [28] (rolling ball background subtraction and Gaussian smoothing). Foci detection was performed using the FociPicker3D ImageJ plugin [29]. An in house developed macro was used to automate the image preprocessing and foci detection. CellProfilerv2.22 [30] was used for nuclei segmentation, counting the number of Bodipy and lysosome foci and establishing parent-child relationships (which foci belong to which cell).

Image analysis results were exported as csv files and read into R (version 3.4.1) for further downstream analysis. Eventually, the fraction of overlapping foci were calculated as compared to total bodipy or lysosomes and normalization of these fractions per number of cells.

Statistical analysis

Bar graphs are expressed as mean ± SD. A two-tailed student's T-test was used to compare individual groups with Gaussian distributed data. Non-parametric data was analyzed using a Mann-Whitney U-test. Data from three or more groups were analyzed using a one-way ANOVA with a subsequent Tukey's multiple comparison test. A p-value

below 0.05 was considered significant. In the figures a * indicates p<0.05, ** indicates p<0.01, *** indicates p<0.001 and **** indicates p<0.0001.

RESULTS

Total and naïve CD4$^+$ T cells accumulate lipids during dyslipidemia

Presumably, Western-type diet (WTD)-induced dyslipidemia in mice increases the amount of lipoproteins to which CD4$^+$ Tn cells are exposed to, as compared to normal chow diet (NCD) fed mice (with normolipidemia). This increase would result in enhanced endolysosomal uptake of lipoproteins and increased lipid droplets (LD) content, despite LXR activation and increased ABC transporter expression.

We examined whether CD4$^+$ Tn cells actually contain more LD when exposed to excess lipoproteins *in vitro* by mimicking dyslipidemia with atherogenic lipoproteins. Alternatively, dyslipidemia was mimicked using serum from WTD-fed mice and compared to NCD-serum control, to mimic lipoprotein excess in the context of inflammatory factors associated with dyslipidemia-induced atherosclerosis.

First, we incubated isolated CD4$^+$ Tn cells with the atherogenic lipoproteins oxLDL and VLDL, which mimic hypercholesterolemia and hypertriglyceridemia, respectively, and assessed LD accumulation through flow cytometry. OxLDL and VLDL increased the median fluorescent intensity (MFI) of Bodipy, a neutral lipid dye which can stain LD, in CD4$^+$ Tn cells as compared to control incubated T cells (fig. 1A). Similar to incubation with isolated oxLDL and VLDL, incubating CD4$^+$ Tn cells with serum from WTD-fed *Ldlr*$^{-/-}$ resulted in a higher LD stain as compared to serum from NCD-fed *Ldlr*$^{-/-}$ mice (fig. 1B).

To confirm that dyslipidemia is indeed associated with increased LD content and LXR activation *in vivo*, we examined whether CD4$^+$ T cells have enhanced LD formation during dyslipidemia. To this end, we fed *Ldlr*$^{-/-}$ mice a Western-type diet (WTD) containing 0.25% cholesterol and 15% cocoa butter for 4 weeks to induce dyslipidemia and quantified the degree of LD formation in isolated CD4$^+$ T cells. CD4$^+$ T cells isolated from WTD-fed mice more frequently contained one or more LD than CD4$^+$ T cells from normal chow diet (NCD) fed control mice (fig. 1C). In line, the mRNA expression of *Plin2*, which is involved in LD formation, was increased in CD4$^+$ T cells from WTD-fed mice (fig. 1D). *CD36* mRNA expression was not modulated by WTD (fig. 1E) suggesting that prolonged exposure of CD4$^+$ T cells to excess lipoproteins did not result in downregulation of scavenger receptors which mediate the uptake of lipoproteins, comparable to lipid loaded macrophages [31]. Actually, we have shown that CD36 expression on a protein level is increased in conventional CD4$^+$ T cells isolated from *Ldlr*$^{-/-}$ mice with diet-induced dyslipidemia, as compared to normolipidemic mice (J. Amersfoort, unpublished).

In $CD4^+$ T cells from WTD-fed mice we determined, however, an increased mRNA expression of *Abca1* which encodes the ABCA1 cholesterol efflux transporter but not of *Abcg1* (fig 1F), indicating that LXR is activated in $CD4^+$ T cells *in vivo* by dyslipidemia. Next, we assessed whether there are dynamic changes in LXR activation in $CD4^+$ T cells during prolonged WTD-induced dyslipidemia. Again, the mRNA expression of *Abca1* was elevated after 4 weeks of WTD as compared to the NCD controls (fig. 1G). Moreover, it remained increased after 8 and 16 weeks of WTD to a similar extent suggesting that LXR remained elevated during prolonged WTD feeding. The expression of *Abcg1* was significantly increased after 4 weeks of WTD as compared to the NCD control, but did not remain significantly higher at 8 and 16 weeks of WTD (fig. 1H). To establish that the increase in *Abca1* and *Abcg1* was LXR-dependent, we isolated $CD4^+$ T cells and mimicked dyslipidemia *in vitro* using human VLDL and simultaneously treated the cells with the LXR antagonist GSK2033. *Abca1* and *Abcg1* expression was almost abolished in GSK2033 treated $CD4^+$ T cells (fig. 1I), suggesting that *Abca1* and *Abcg1* expression in CD4+ T cells in the presence of excess atherogenic lipoproteins is LXR-dependent.

Altogether, these results indicated that WTD-induced dyslipidemia induced lipid accumulation in total $CD4^+$ T cells and an LXR-dependent increase in the expression of cholesterol efflux transporters and that dyslipidemia-like conditions induced lipid accumulation in $CD4^+$ Tn cells *in vitro*.

Priming of $CD4^+$ Tn cells with isolated lipoproteins increases proliferation of antibody- but not antigen-stimulated T cells

As we were interested in the priming of $CD4^+$ Tn cell by lipoproteins, we isolated $CD4^+$ Tn cells, induced lipid loading *in vitro* using oxLDL and VLDL and subsequently studied cell growth and proliferation after TCR stimulation with antibodies or antigen (fig. 2A). We used suboptimal antibody-induced TCR stimulation (1 µg/mL plate-bound αCD3) as we reasoned that any dyslipidemia-mediated effects on proliferation would be less apparent during strong TCR stimulation. Alternatively, we assessed proliferation in response to strong, antigen-induced TCR stimulation, which has the advantage that bone marrow-derived dendritic cells (BMDC) provide a more physiological co-stimulatory signal and cytokine stimulation of primed $CD4^+$ Tn cells.

We also studied the effect of lipoprotein-induced priming by activating the cells in the absence or presence of oxLDL and VLDL. We hypothesized that the cell blast (or cell growth) phase which precedes cell division within 24 hours after antibody-induced activation [32] is increased after lipoprotein-induced priming of $CD4^+$ Tn cells. However, T cell blast after 18 hours of activation was not affected by lipoprotein-induced priming since the cell size, which was measured by the forward scatter (FSC), was not enhanced in the primed $CD4^+$ T cells as compared to the vehicle-treated $CD4^+$ T cells. (fig. 2B). Interestingly, T cell blast was diminished when $CD4^+$ Tn cells were activated in the pres-

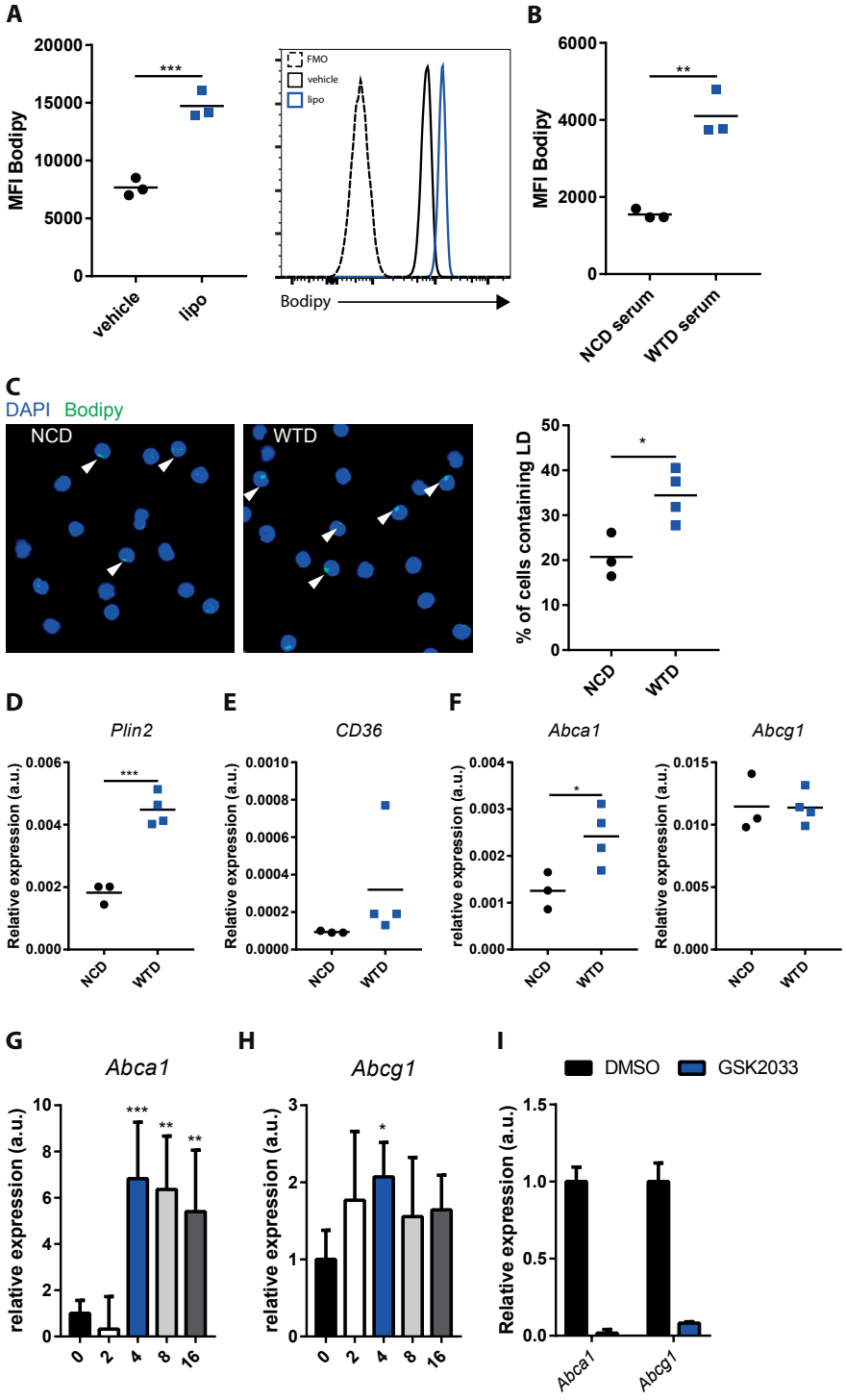
A
MFI Bodipy
20000
15000
10000
5000
0
***
vehicle
lipo
FMO
vehicle
lipo
Bodipy
B
MFI Bodipy
6000
4000
2000
0
**
NCD serum
WTD serum
C
DAPI Bodipy
NCD
WTD
% of cells containing LD
50
40
30
20
10
0
*
NCD
WTD
D
Plin2
Relative expression (a.u.)
0.006
0.004
0.002
0.000
***
NCD
WTD
E
CD36
Relative expression (a.u.)
0.0010
0.0008
0.0006
0.0004
0.0002
0.0000
NCD
WTD
F
Abca1
relative expression (a.u.)
0.004
0.003
0.002
0.001
0.000
*
NCD
WTD
Abcg1
Relative expression (a.u.)
0.015
0.010
0.005
0.000
NCD
WTD
G
Abca1
relative expression (a.u.)
10
8
6
4
2
0
***
**
**
0
2
4
8
16
H
Abcg1
relative expression (a.u.)
3
2
1
0
*
0
2
4
8
16
I
DMSO
GSK2033
Relative expression (a.u.)
1.5
1.0
0.5
0.0
Abca1
Abcg1

Figure 1 CD4$^+$ T cells from *Ldlr*$^{-/-}$ mice accumulate lipids *in vivo* and *in vitro* which elicits an LXR response. (A) Quantification of Bodipy median fluorescent intensity (MFI) in CD4$^+$ T cells loaded with lipoproteins (lipo) *in vitro*. (B) Quantification of LD MFI in Tn cells incubated *in vitro* with serum from NCD- or WTD-fed mice. (C) The percentage of T cells containing LD as assessed by confocal microscopy. (D) *Plin2* expression in isolated CD4+ T cells. (E) *CD36* expression in isolated CD4$^+$ T cells. (F) *Abca1* and *Abcg1* expression in isolated CD4$^+$ T cells. (G) Expression of *Abca1* in T cells from mice fed a normal chow diet (NCD, t=0) or a WTD for 2-16 weeks. (H) Expression of *Abcg1* in same experiment. (I) Expression of *Abca1* and *Abcg1* after LXR inhibition with GSK2033 *in vitro* in the presence of atherogenic lipoproteins. Asterisks in 1G and 1H indicate a significant difference as compared to 0 weeks WTD. White arrows in 1C indicate a CD4$^+$ T cell with LD.

ence of lipoproteins, independent of the priming condition. We also measured CD4$^+$ T cell activation as reflected by the percentage of IL-2 producing CD4$^+$ T cells after 18 hours of antibody-induced activation. In line with equal cell growth between vehicle- and lipoprotein-primed CD4$^+$ T cells, the percentage of IL-2$^+$ cells within the CD4$^+$ T cell population was equal between vehicle- and lipoprotein-primed T cells (fig. 2C). Activation of CD4$^+$ Tn cells in the presence of lipoproteins also reduced the percentage of IL-2 producing CD4$^+$ T cells. Besides the effect of priming on T cell activation, we wanted to examine the effect of lipoprotein-induced priming on the proliferation of CD4$^+$ T cells. To this end, we activated CD4$^+$ Tn cells for 72 hours with αCD3 and αCD28 antibodies as initial cell division occurs after approximately 48 hours after TCR stimulation and priming effects might be diluted after longer stimulation. Interestingly, lipoprotein-induced priming of CD4$^+$ Tn cells increased the percentage of proliferated cells after 72 hour of antibody-induced TCR stimulation but this effect of lipoprotein-induced priming was abolished when the cells were activated in the presence of excess lipoproteins (fig. 2D). Furthermore, activation of vehicle-primed CD4$^+$ Tn cells in the presence of excess lipoproteins increased the percentage of proliferated cells as compared to CD4$^+$ T cells activated without excess lipoproteins. The effects of lipoprotein-induced priming and activation of CD4$^+$ Tn cells in the presence of excess lipoproteins were reflected by the percentage of IL-2 producing CD4$^+$ T cells after 72 hour stimulation (fig. 2E).

Next, we wanted to assess the effect of lipoprotein-induced priming on T cell proliferation by activating CD4$^+$ Tn cells in an antigen-specific manner. To this end, we induced proliferation of primed OT-II T cells in a co-culture of these cells with BMDC which were previously loaded with various concentrations of OVA-323 peptide. We did not include a condition in which we activated vehicle- or lipoprotein-primed CD4$^+$ OT-II T cells in the presence of excess lipoproteins as lipoprotein uptake by BMDCs induces phenotypic changes, leading to enhanced activation of T cells [33]. Moreover, lipoprotein-induced priming was counteracted by the presence of excess lipoproteins during antibody-induced activation of CD4$^+$ T cells, suggesting that activation in the context of dyslipidemia might mask any priming effect which we were interested in. Lipoprotein-induced

priming of CD4$^+$ Tn cells did not enhance the antigen-induced proliferation of OT-II cells as compared to vehicle-induced priming (fig. 2F).
Altogether, these data showed that priming of CD4$^+$ Tn cells with lipoproteins enhanced proliferation after suboptimal, antibody-induced T cell activation but not after antigen-induced T cell activation.

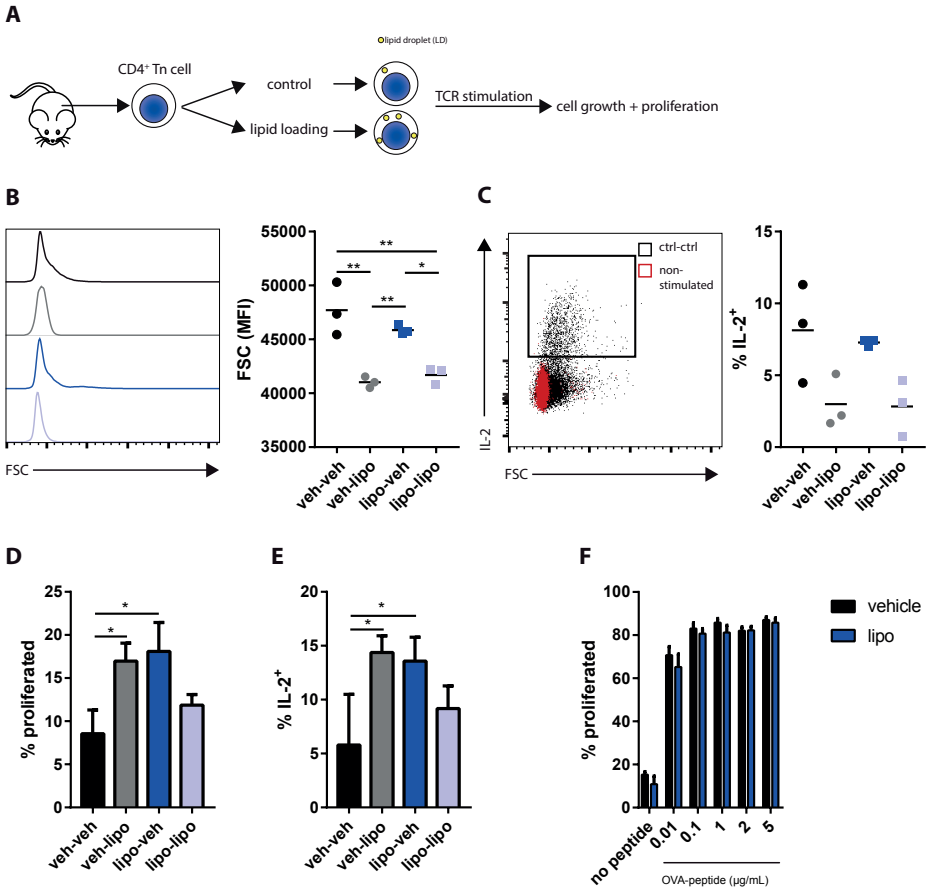

Figure 2 Lipoprotein-induced priming of CD4$^+$ *Ldlr*$^{-/-}$ Tn enhanced proliferation in response to antibody-mediated TCR stimulation. (A) Experimental setup for *in vitro* evaluation of effect of CD4$^+$ Tn cell priming on proliferation. (B) Cell growth as assessed by flow cytometry (median fluorescent intensity, MFI) after 18 hours of antibody-induced T cell activation. (C) Percentage of IL-2 producing CD4$^+$ T cells after 18 hours of antibody-induced T cell activation. (D) Proliferation after 72h stimulation with antibody-induced T cell activation. (E) Percentage of IL-2 producing CD4$^+$ T cells after 72 hours of antibody-induced T cell activation. (F) Antigen-induced proliferation of OT-II T cells in a co-culture with BMDC as measured by CellTrace dilution. Groups in B-E are indicated as priming condition-activating condition, thus, veh-lipo indicates vehicle-primed T cells which are activated in the presence of excess lipoproteins.

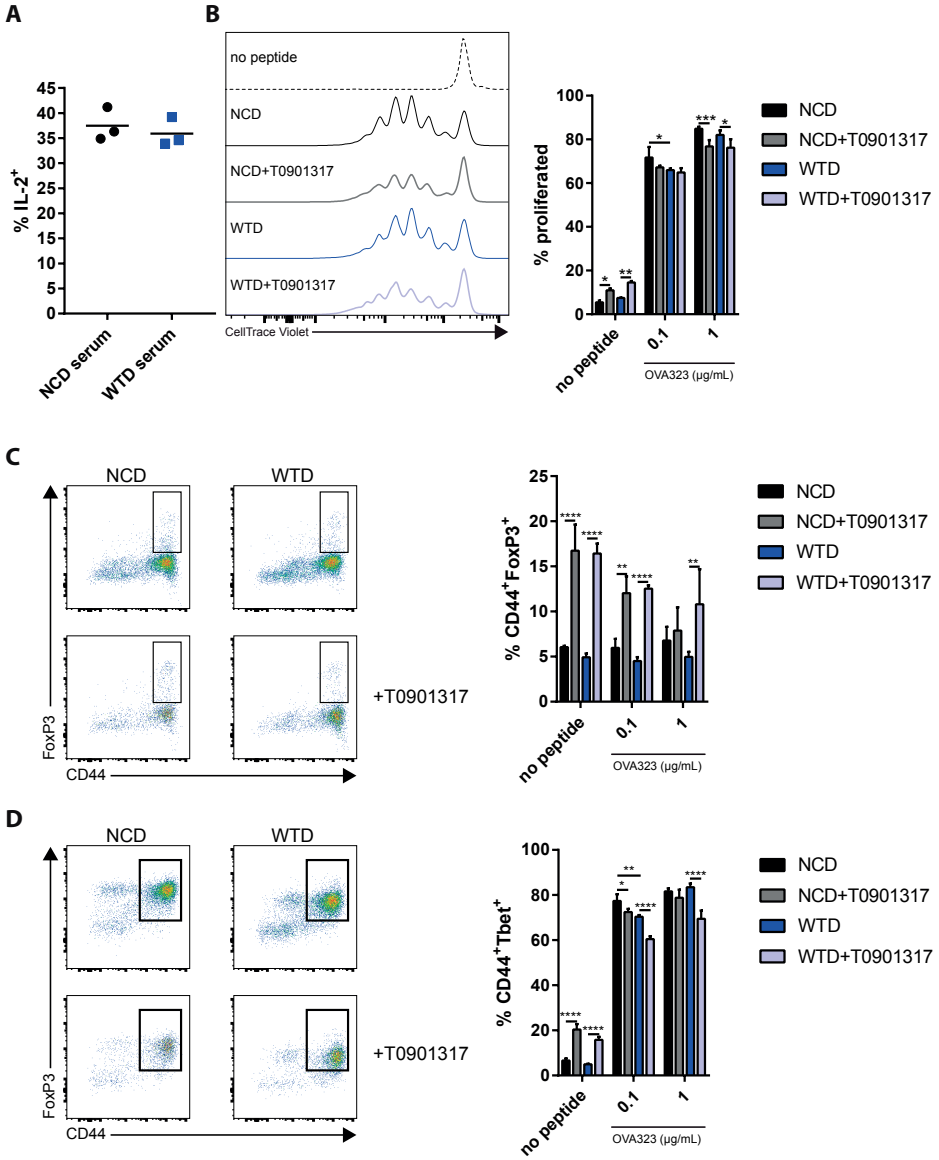

Figure 3 Pharmacological LXR activation during the priming of CD4$^+$ Tn cells with WTD-serum decreased proliferation and promoted Treg cell differentiation. (A) Percentage of IL-2 producing CD4$^+$ T cells after 18 hours incubation of OT-II CD4$^+$ Tn cells with BMDCs loaded with various concentrations of OVA323. (B) Antigen-induced proliferation as assessed by CellTrace dilution after 96 hours of incubation with indicated preceding priming conditions. (C) Treg cell percentage after 96 hours of incubation. (D) Th1 cell percentage after 96 hours of incubation.

LXR activation during WTD serum-induced priming of CD4$^+$ Tn cells has anti-inflammatory effects

Since LXR activation and Abcg1 are crucial factors during T cell proliferation and differentiation and lipid accumulation in T cells induced LXR activation, we postulated that activation of LXR in CD4$^+$ Tn cells under dyslipidemic conditions would affect their effector phenotype.

Therefore, we primed CD4$^+$ Tn cells with NCD- or WTD-serum with or without the addition of the LXR agonist T0901317 and assessed the proliferation and Treg/Th1 differentiation after antigen-stimulation. After 18 and 96 hours of antigen-induced CD4$^+$ T cell activation, no difference in the percentage of IL-2 producing cells was observed between NCD- and WTD-serum primed CD4$^+$ T cells (fig. 3A,B). Interestingly, activation of LXR with T0901317 during priming slightly decreased the percentage of proliferated CD4$^+$ T cells, which is in line with previous reports describing LXR-agonists to suppress T cell proliferation [6]. In the same experiment, we also assessed the effect of serum-priming on the differentiation skewing of CD4$^+$ T cells. Again, no difference in the percentage of Treg cells was observed after priming with WTD-serum as compared to NCD-serum (fig. 3C). Interestingly, 48 hours of priming with T0901317 did increase the percentage of Treg cells (as defined by CD44$^+$FoxP3$^+$ cells in the CD4$^+$ population) in the presence of both NCD- and WTD-serum. T0901317 also increased the percentage of Treg cells when OT-II CD4$^+$ T cells were incubated with unloaded BMDCs, suggesting that part of the Treg cell simulating effect of T0901317 was OVA323 independent. Furthermore, T0901317 treatment specifically during the priming of CD4$^+$ Tn cells with WTD-serum reduced the percentage of Th1 cells (as defined by CD44$^+$Tbet$^+$ cells in the CD4$^+$ population) as compared to CD4$^+$ which were primed with only WTD-serum (fig. 3D). Altogether, these results indicated that priming of CD4$^+$ Tn cells with WTD-serum did not affect T cell proliferation or differentiation but T0901317 treatment under dyslipidemia-like conditions inhibited proliferation and skewed CD4$^+$ T cell differentiation to Treg cells.

WTD-induced dyslipidemia does not induce autophagy in CD4$^+$ T cells

As acetylated-LDL induces lipophagy in foam cells [25] we aimed to examine whether dyslipidemia induced lipophagy in CD4$^+$ T cells as well. This is relevant as this would affect the outcome of stimulation or inhibition of autophagy on lipid accumulation during the priming of CD4$^+$ Tn cells under dyslipidemia-like conditions. To this end, we fed *Ldlr*$^{-/-}$ mice a WTD for 4 weeks, isolated CD4$^+$ T cells and compared the level of autophagy to CD4$^+$ T cells from NCD-fed mice. An immunoblot for LC3 showed that the amount of lipidated LC3 (LC3-II, indicating active autophagy) was equal between CD4$^+$ T cells from NCD- and WTD-fed mice (fig. 4A). Another method to quantify active autophagy is by measuring the amount of LC3 puncta through confocal microscopy as LC3 puncta reflect matured autophagosomes [34]. The percentage of cells which contained LC3 puncta

did not differ between $CD4^+$ T cells isolated from NCD- and WTD-fed mice (fig. 4B). This suggested that diet-induced dyslipidemia prompted lipid accumulation in $CD4^+$ T cells but not severe enough to induce autophagy. In addition, as autophagy is not induced by dyslipidemia, lysosomal inhibition during the priming of $CD4^+$ Tn cells mostly inhibits the endolysosomal uptake of lipoproteins and not lipophagy-mediated LD degradation.

Chloroquine inhibits serum-induced lipid accumulation

Chloroquine inhibits LAL, thereby impairing the degradation of cholesteryl esters and triglycerides and formation of LD as well as autophagy-mediated degradation of LD (i.e. lipophagy). To assess whether chloroquine would inhibit the endolysosomal uptake of lipoproteins during dyslipidemia-like priming conditions, we isolated $CD4^+$ Tn cells and incubated them with chloroquine 2 hours prior to and during priming with NCD- and WTD-serum to induce lipid accumulation as compared to a medium control. To quantify whether chloroquine induces lipid accumulation in lysosomes, we performed a proof-of-principle experiment where we stained neutral lipids (esterified lipids and choles-

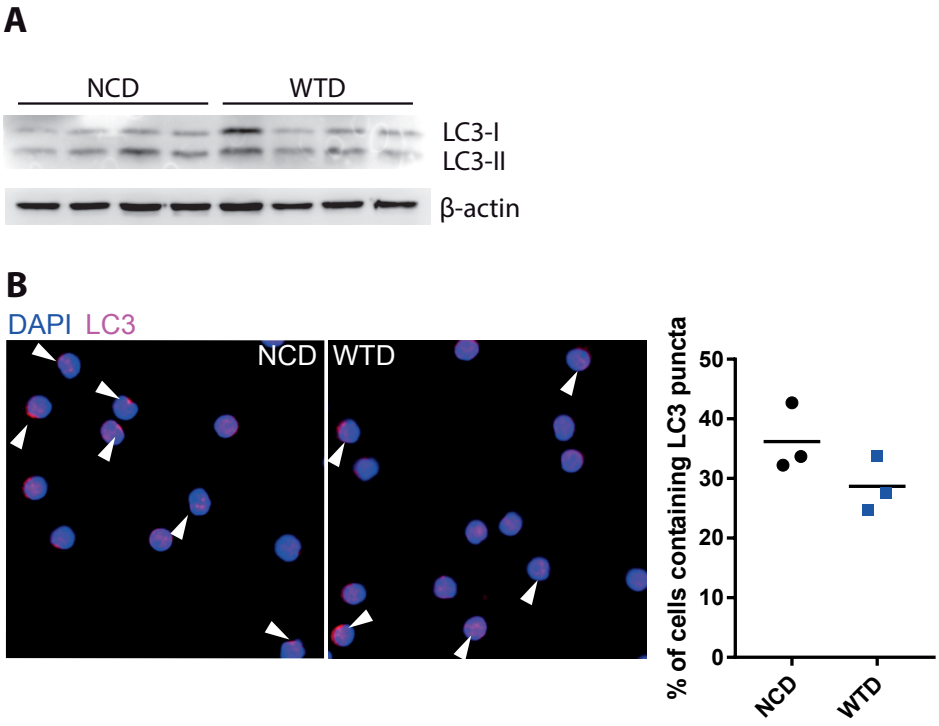

Figure 4 Diet-induced dyslipidemia did not induce autophagy in $CD4^+$ T cells. (A) Immunoblot showing LC3-I and LC3-II (the lipidated LC3 indicating active autophagy) in CD4+ T cells derived from NCD or WTD fed mice (n=4/group). (B) Assessment of lipophagy by quantification of the percentage of $CD4^+$ T cells with LC3 puncta as a measure for active autophagy. White arrows indicate cells with clear LC3 puncta.

terol) and lysosomes using Bodipy and Lysotracker, respectively, and used automated segmentation of neutral lipid- and lysosome foci in <150 $CD4^+$ Tn cells per condition. $CD4^+$ Tn cells incubated with NCD- and WTD-serum for 24 hours showed an increase in the number of neutral lipid foci per cell which was inhibited by incubating the cells with chloroquine 2 hours prior to and during the 24 hours priming (fig. 5A). As chloroquine also inhibits the fusion between endosomes and lysosomes [35], chloroquine treatment likely decreased the level of lipoprotein handling through several mechanisms in $CD4^+$ Tn cells and thus decreased the formation of LD. The fraction of neutral lipid foci which colocalize with lysosomes, after normalization to the number of lysosomes and cells, was increased in the chloroquine treated condition (fig. 5B). This was especially apparent in the WTD-serum primed $CD4^+$ Tn cells (fig. 5C). Since dyslipidemia did not result in the induction of autophagy, increased colocalization between neutral lipid foci and lysotracker foci is likely due to lipid accumulation in lysosomes. Naturally, it cannot be ruled out that chloroquine treatment impaired the autophagic degradation of LD which would also result in enhanced colocalization between neutral lipid- and lysosome foci. Automated segmentation of neutral lipid foci (fig. 5D) and lysosomes (fig. 5E) resulted in a slight overestimation of the number of foci, as indicated by segments of lysosomes in the absence of a clear lysosome signal. Nevertheless, a proof-of-principle experiment showed that automated segmentation is suitable to identify neutral lipid and lysosome foci in confocal images of $CD4^+$ Tn cells which suggested that chloroquine impaired the endolysosomal uptake and degradation of lipids and formation of lipid droplets under dyslipidemia-like priming conditions.

Lysosomal inhibition while priming naïve T cells with serum inhibits T cell activation

Priming of $CD4^+$ Tn cells under dyslipidemia-like conditions had minor effects on the effector phenotype of $CD4^+$ T cells as shown in figure 2 and 3. Interestingly, promoting cholesterol efflux with an LXR-agonist during priming did have minor anti-inflammatory effects as it slightly inhibited proliferation of $CD4^+$ T cells and promoted Treg cell differentiation. To further explore whether inhibiting the availability of free cholesterol through lysosomal inhibition would have similar anti-inflammatory effects we treated $CD4^+$ Tn cells during priming with chloroquine. In $CD4^+$ Tn cells primed with WTD serum, chloroquine treatment significantly inhibited T cell activation as measured by the percentage of IL-2 producing cells after overnight activation with antibody-induced TCR stimulation (fig. 6A). Perhaps this is because fewer lipids can be taken up through the endolysosomal pathway as well as decreased LD degradation via lipophagy. In line, proliferation showed a strong trend ($p=0.0506$) towards being decreased in chloroquine treated WTD-serum primed T cells activated for 72 hours (fib. 6B). To assess the effect of autophagy inhibition on the differentiation status of T cells, we measured the percentage of Treg and Th1 cells

after 72 hours activation. No effects were observed on the percentage of Treg cells, while Th1 cells were decreased in Tn cells primed with WTD-serum and chloroquine as compared to WTD-serum primed Tn cells (fig. 6C). These *in vitro* results suggested that the decrease in cholesterol availability after lysosomal inhibition, which limits the uptake of lipoproteins from the environment as well as the degradation of LD through autophagy, in the initial phase of T cell activation might have anti-inflammatory effects. Proliferation and Th1 differentiation was severely impaired after chloroquine treatment during WTD-serum priming, which is in line with literature describing pharmacological inhibition of autophagy to inhibit proliferation of Th1 cells [36]. To explore the therapeutic potential of chloroquine to inhibit T cell-mediated inflammation we fed mice a NCD or a WTD for 4 weeks and treated them with chloroquine for three consecutive days and assessed the percentage of Treg- and Th1 cells in the spleen. Surprisingly, chloroquine actually increased the percentage of Treg cells in WTD-fed mice but not in NCD-fed mice (fig. 6D) while we did not observe any effect of chloroquine treatment on the percentage of Th1 cells (fig. 6E). Moreover, we did not observe an anti-proliferative effect of chloroquine on T cells as the percentage of proliferating cells was elevated in chloroquine-treated mice fed a WTD (fig. 6F).
In conclusion, these data suggest that lysosomal inhibition with chloroquine might have anti-inflammatory effects on T cells specifically during dyslipidemia and dyslipidemia-like conditions.

DISCUSSION

Dyslipidemia has been shown to have lipid-mediated antigen-independent effects on T cell effector function in atherosclerosis. Moreover, autophagy-induced degradation of LD is an essential metabolic process in foam cells which facilitates cholesterol efflux. However, it is unknown whether atherogenic lipoproteins prime $CD4^+$ Tn cells to have an altered effector phenotype, and whether lipid-associated metabolic processes contribute to the priming effect. Through *in vitro* and *in vivo* studies we showed that dyslipidemia and dyslipidemia-like conditions affect lipid metabolism in $CD4^+$ T cells but that pharmacological modulation of lipid metabolism in $CD4^+$ Tn cells had the largest immunomodulatory effect specifically under dyslipidemic conditions.
First we showed that $CD4^+$ T cells accumulate lipids in *Ldlr*$^{-/-}$ mice fed a WTD as compared to NCD-fed controls. This was reflected by an increase in the mRNA expression of ABCA1 and ABCG1 in T cells in an LXR-dependent manner and increased *Plin2* expression. Further characterization of the content of LD and how dietary lipids affect their content should shed more light on the exact functional implications of LD accumulation and expansion in T cells. In macrophages and dendritic cells, different types of LD exist within

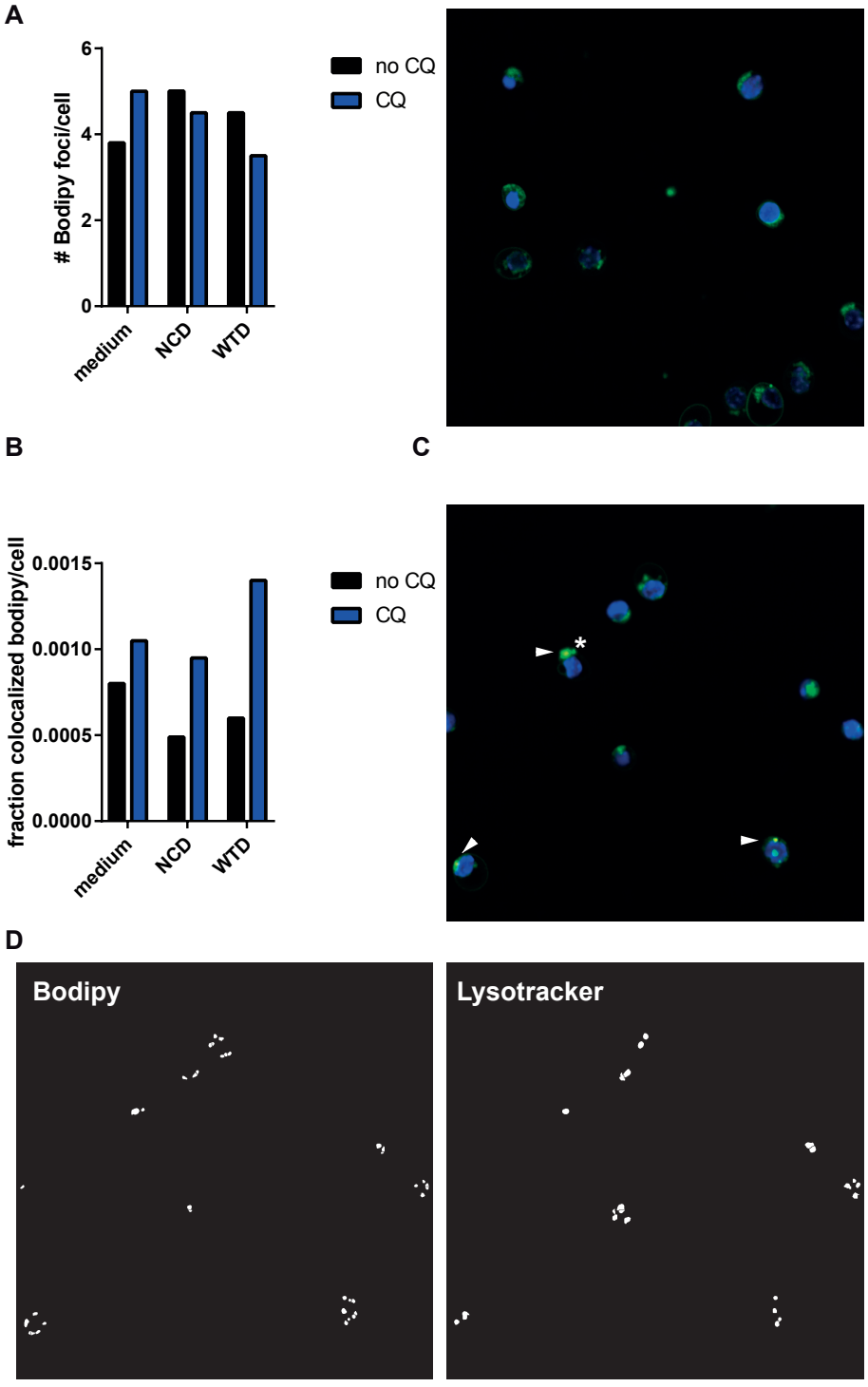
A
Bodipy foci/cell
6
4
2
0
medium
NCD
WTD
no CQ
CQ
B
fraction colocalized bodipy/cell
0.0015
0.0010
0.0005
0.0000
medium
NCD
WTD
no CQ
CQ
C
D
Bodipy
Lysotracker

Figure 5 Chloroquine inhibits endolysosomal processing of lipoproteins and impairs serum-induced lipid accumulation. (A) Quantification of Bodipy-stained lipid droplets as detected by automated segmentation in indicated treatments. An example of Bodipy stained lipid droplets is shown. (B) Colocalization between lipid droplets and lysosomes (stained with Lysotracker-RED DND-99) by automated segmentation in indicated treatments. (C) Example of immunofluorescent image of lipid droplets and lysosomes in WTD-serum and chloroquine primed $CD4^+$ Tn cells. White arrows indicate colocalization between lipid droplet and lysosome in yellow. An asterisk indicates a lipid droplet (D) Corresponding images showing neutral lipid foci and lysosome segments in white. CQ indicates chloroquine.

individual cells [37]. Moreover, it has been shown that different types of LD can affect various intracellular processes involved in inflammation, including IFN-signaling, cross presentation and bioenergetic metabolism [38]. LD are also involved in the metabolism of arachidonic acid and its metabolites, eicosanoids [38,39]. Some eicosanoids are potent immunological mediators and are potent ligands for peroxisome proliferator activated receptor delta, which mediates altered cellular metabolism in Treg cells during dyslipidemia (J. Amersfoort et al., unpublished). Therefore, although we did not observe any major effects of priming of $CD4^+$ Tn cells using human serum-derived lipoproteins or WTD-serum, a different method of priming could induce distinct types of LD which could modulate the inflammatory phenotype of effector $CD4^+$ T cells. A recent report described that mitochondria-associated LD have unique bioenergetics properties, dynamics and composition [40]. These reports suggest that LD have the potential to modulate T cell metabolism and therefore effector function and call for the characterization of the different types of LD present in T cells from patients with dyslipidemia and cardiovascular disease. Lipid accumulation in $CD4^+$ T cells was not associated with increased autophagy, as opposed to foam cells [25]. This was surprising as cholesterol accumulation in Treg cells is associated with decreased mTORC1 activity during diet-induced dyslipidemia [11] and mTORC1 inhibits autophagy by phosphorylating Ulk1 [41]. Given that scavenger receptors mediate the uptake of (modified) lipoproteins [42,43], perhaps scavenger receptor expression or cytoplasm volume in $CD4^+$ Tn cells is too low to induce lipid accumulation to an extent which requires autophagy induction to facilitate reverse cholesterol transport and prevent lipotoxicity. As Treg cells appear to have higher lipid scavenging capacity than conventional T cells (J. Amersfoort et al., unpublished), dyslipidemia might induce autophagy in Treg cells. Importantly, this does not mean that lipophagy is not involved in the inflammatory effects of lipid-mediated priming of Tn cells. Lipophagy-mediated degradation of LD could enhance the availability of cholesterol and other lipids in the initial stage of T cell activation and affect their effector phenotype under inflammatory conditions which we did not examine. Of note, chloroquine inhibits atherosclerosis in apolipoprotein-E deficient mice in a p53-dependent manner [44]. p53 is a tumor suppressor protein which induces apoptosis and has been described to inhibit cholesterol synthesis [45], suggesting that chloroquine could impair T cell-mediated inflammation by

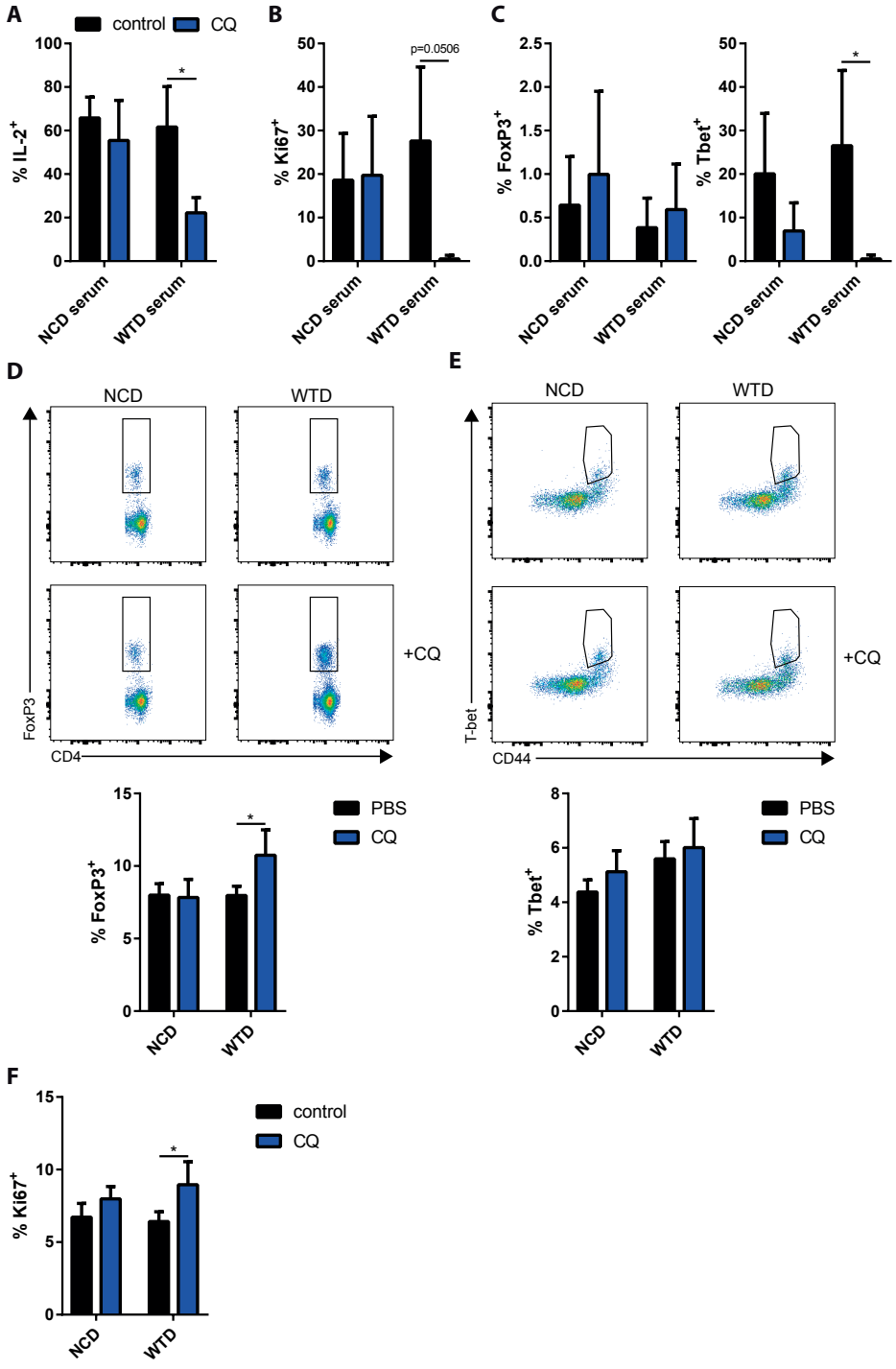
A
control
CQ
% IL-2+
NCD serum
WTD serum
B
% Ki67+
p=0.0506
C
% FoxP3+
% Tbet+
D
NCD
WTD
+CQ
FoxP3
CD4
% FoxP3+
PBS
CQ
E
T-bet
CD44
% Tbet+
F
% Ki67+

Figure 6 Lysosomal inhibition during WTD serum priming inhibits activation and proliferation. (A) IL-2 production after ON activation of $CD4^+$ T cells primed as indicated. (B) $CD4^+$ T cell proliferation of primed $CD4^+$ T cells after 72h of activation. (C) Percentage of Treg- and Th1 cells in same experiment as in (B). (D) Percentage of Treg cells in splenic $CD4^+$ population in *Ldlr*$^{-/-}$ mice on a NCD or WTD treated with control (PBS) or chloroquine. (E) Percentage of Th1 cells in same experiment as in D. (F) Percentage of proliferating $CD4^+$ T cells in same experiment as in D. CQ indicates chloroquine.

decreasing cholesterol-synthesis. These data underline the therapeutic possibility of using chloroquine or chloroquine-diphosphate to inhibit T cell-mediated inflammation in atherosclerosis.

Priming of $CD4^+$ Tn cells with atherogenic lipoproteins induced lipid accumulation in $CD4^+$ Tn cells *in vitro* but did not increase cell growth after overnight antibody-induced activation. However, both priming of naïve T cells with lipoproteins as activating unprimed (vehicle control) $CD4^+$ Tn cells in the presence of lipoproteins enhanced their proliferation in response to prolonged stimulation. Activation of $CD4^+$ T cells in the presence of oxLDL and VLDL decreased the percentage of IL-2 producing $CD4^+$ T cells. This reduction of T cell blast and IL-2 production is in line with a report describing human T cells proliferate less when activation occurs in the presence of 10 ug/mL oxLDL [46]. Interestingly, priming with lipoproteins did not enhance the antigen-specific proliferation after 96 hours incubation of OT-II T cells with OVA323 loaded BMDCs, suggesting the priming of $CD4^+$ Tn cells with lipoproteins has stimulation-dependent effects on proliferation. Another explanation is that antigen-specific proliferation was not enhanced in primed OT-II T cells but was enhanced in *Ldlr*$^{-/-}$ T cells which were activated using antibody-stimulation, is the presence of a functional LDL receptor. In $CD4^+$ T cells isolated from transgenic OT-II mice, LDL receptor-mediated uptake of native lipoproteins could have overruled the priming effect.

Priming $CD4^+$ Tn cells with normolipidemic or dyslipidemic serum did not affect antigen-specific proliferation either. This could be because the affinity of the OVA323-peptide for the TCR of OT-II T cells is higher than the affinity of physiological antigens, such as ApoB100 derived-peptides. Hence, priming of $CD4^+$ Tn cells might be overruled by strong TCR signals which enhance the transcriptional program facilitating cell growth and proliferation. Priming might only affect proliferation during suboptimal stimulation, as was the case in the antibody-stimulation which we used.

Enhanced cholesterol content in T cells is generally associated with elevated proliferation by enhancing the availability of cholesterol for membrane synthesis and fine-tuning the TCR [47]. However, the modulatory effect of cholesterol on TCRs is not as straightforward as suggested by reports describing cholesterol to enhance the nanoclustering of TCRs [48] and free cholesterol to enhance TCR signaling in $CD8^+$ T cells [20]. The activity of Sult2b, which inactivates oxysterols as LXR ligands through sulfation, might negatively modulate cholesterol-mediated enhancement of TCR signaling. Moreover, cholesterol

binding to the TCRβ subunit has been shown to both drive TCR dimerization and avidity to MHC-peptide complex as inhibit spontaneous TCR signaling [49]. Promoting cholesterol efflux with an LXR agonist during dyslipidemia-like priming slightly decreased antigen-specific proliferation. Upon TCR stimulation, T cells acquire a transcriptional program which drives cholesterol synthesis, in part by increasing the expression of Sult2b1 [6]. Moreover, during the blasting phase, but not during the cell division phase, lipid synthesis is increased in a SREBP-dependent manner [7]. Presumably, LXR agonism during priming of $CD4^+$ Tn cells did not inhibit their antigen-induced proliferation in a major way because cholesterol synthesis is induced to such an extent that the effects of LXR agonism on proliferation are overruled.

Inducing cholesterol efflux during priming by treating $CD4^+$ Tn cells with T0901317 enhanced the generation of Treg cells and decreased Th1 differentiation after antigen-induced activation. The former is in line with a report describing LXR activation with GW3965 to promote differentiation of $CD4^+$ T cells towards Treg cells [50]. Interestingly, another report by Takeuchi et al. suggested that pharmacological activation of retinoid-X-receptor, the protein with which LXR forms a heterodimer [51], promotes the differentiation of $CD4^+CD25^-$ to Treg cells but LXR agonism alone using T0901317 does not [52]. The Treg cells in those reports were mainly generated *in vitro* using antibodies and transforming growth factor β1, which is a common method to generate Treg cells from murine $CD4^+$ T cells. In our T cell-BMDC co-culture, Treg cell differentiation was likely induced by the BMDC-derived cytokines after T0901317 was washed away after the preceding priming step. Therefore, these results support the notion that modulation of cholesterol metabolism only during the priming of $CD4^+$ Tn cells with dyslipidemic serum can induce T cell skewing. Whereas LXR agonism enhanced Treg cell differentiation under normolipidemia- and dyslipidemia-like conditions, it inhibited Th1 cell differentiation only under dyslipidemia-like conditions. LXR agonists have been described to inhibit IFNγ secretion in murine [50] and human T cells [53]. Again, in our experimental setup, LXR activation was mainly exerted in the priming phase as it was washed away prior to the activation of OT-II T cells. Altogether, the presented study suggests that promoting the efflux of cholesterol in $CD4^+$ Tn cells under dyslipidemia-like conditions affects T cell skewing in the effector phase.

Finally, we assessed whether modulation of lipid metabolism through chloroquine-induced lysosomal inhibition under dyslipidemia-like priming conditions affects T cell proliferation and skewing in a manner similar to LXR activation. Chloroquine treatment decreased T cell activation specifically under dyslipidemia-like conditions as shown by a decrease in the percentage of IL-2 producing T cells after overnight antibody-induced activation. Moreover, chloroquine treatment reduced the percentage of proliferating T cells after 72 hours of stimulation, specifically under dyslipidemia-like priming conditions. Treg cell differentiation was not altered as adequate Treg cell differentiation *in*

vitro requires addition of TGFβ [54] or weak TCR stimulation [55]. However, in line with LXR activation, which reduces intracellular cholesterol content and Th1 differentiation, chloroquine pre-treatment decreased the percentage of Th1 cells after 72 hours of stimulation. This suggests that lysosomal inhibition could prove useful to alter the effector T cell phenotype by altering lipid metabolism of Tn cells. In line, lysosomal inhibition using chloroquine inhibits the activity of LAL, which decreases ABCA1 expression in fibroblasts [56], suggesting that lysosomal inhibition decreases the intracellular oxysterol abundance. Accordingly, fibroblasts isolated from patients with cholesteryl ester storage disease, which have impaired LAL activity, have impaired upregulation of *Abca1* expression in response to LDL loading [56]. *In vivo*, chloroquine did enhance the percentage of Treg cells in WTD-diet fed mice but had no effect on Th1 cell differentiation and actually increased the percentage of proliferation T cells. These contrasting effects of chloroquine *in vivo*, as compared to *in vitro,* are most likely explained by the effects of chloroquine on APCs as it has been shown to induce tolerogenic DCs in a STAT1-dependent manner [57] and can inhibit experimental autoimmune encephalomyelitis (EAE) by modulating DCs [58]. Tolerogenic DCs are potent inducers of Treg cells [59]. In the report by Thome et al., systemic treatment with chloroquine enhanced the Treg cell population [58]. Systemic chloroquine treatment does not reduce Th1 differentiation which was surprising as chloroquine has been reported to decrease the secretion of IL-12p40 by DCs, which is a major Th1-inducing cytokine [60]. Moreover, Th1 differentiation is inhibited by chloroquine [61] and proliferation of *in vitro* generated Th1 cells is dampened by the inhibition of autophagy [36]. In our *in vivo* experimental setup, chloroquine might have affected various other immune cell types and non-immune cells which may compensate for the DC-dependent and T cell-specific effects of chloroquine on Th1 cells. Surprisingly, chloroquine treatment in mice with WTD-induced dyslipidemia enhanced the percentage of proliferating $CD4^+$ T cells which is counterintuitive based on reports describing pharmacological and genetic blockade of autophagy to inhibit proliferation [36,62].

Moreover, chloroquine inhibits the antigen processing in DCs and thereby antigen presentation on MHC-I [63] and MHC-II molecules [64]. In line, genetic blockade of autophagy through the knockout of autophagy related protein 7 in DCs inhibits EAE in a T cell expansion-dependent manner [65]. However, chloroquine treatment of DCs during cross presentation actually enhances $CD8^+$ T cell responses suggesting that chloroquine does not have exclusively anti-inflammatory effects on DC function [66]. Therefore, the T cell aspecific effects of *in vivo* chloroquine may explain the observed increase in Ki-67^+ T cells.

Altogether, modulation of lipid metabolism by pharmacological LXR activation or lysosomal inhibition during the priming of $CD4^+$ Tn cells under dyslipidemia-like conditions affects the effector phenotype after antibody- and antigen-induced activation. This suggests that antigen-independent modulation of lipid metabolism in $CD4^+$ Tn cells may

have immunomodulatory effects already prior to activation, which is especially relevant to lymphoid tissue residing T cells. As the effects of priming which we observed were limited, further research is required to fully examine the relevance of the presented findings. Moreover, further mechanistic research is required to further elucidate how specific lipids affect the effector phenotype when modulating lipid metabolism under dyslipidemia-like conditions. Additionally, the relevance of the presented findings to humans with dyslipidemia where physiological antigens stimulate primed $CD4^+$ Tn cells in the presence of excess lipoproteins, should be investigated.

ACKNOWLEDGEMENTS

We thank H. de Bont (Division of Drug Discovery and Safety, LACDR, Leiden University) for his help during the acquisition of confocal microscope images.

REFERENCES

1. Stemme, S. *et al.* T lymphocytes from human atherosclerotic plaques recognize oxidized low density lipoprotein. *Proceedings of the National Academy of Sciences of the United States of America* 92, 3893–3897 (1995).
2. Pierides, C., Bermudez-Fajardo, A., Fredrikson, G. N., Nilsson, J. & Oviedo-Orta, E. Immune responses elicited by apoB-100-derived peptides in mice. *Immunologic research* 56, 96–108 (2013).
3. Emeson, E. E., Shen, M.-L. & Bell, C. G. H. Inhibition of Atherosclerosis in CD4 T-Cell-Ablated and Nude (nu/fu) C57BL/6 Hyperlipidemic Mice. 149, 11 (1996).
4. Pearce, E. L., Poffenberger, M. C., Chang, C.-H. & Jones, R. G. Fueling immunity: insights into metabolism and lymphocyte function. *Science (New York, N.Y.)* 342, 1242454 (2013).
5. Ron-Harel, N. *et al.* Mitochondrial Biogenesis and Proteome Remodeling Promote One-Carbon Metabolism for T Cell Activation. *Cell Metabolism* 24, 104–117 (2016).
6. Bensinger, S. J. *et al.* LXR Signaling Couples Sterol Metabolism to Proliferation in the Acquired Immune Response. *Cell* 134, 97–111 (2008).
7. Kidani, Y. *et al.* Sterol regulatory element-binding proteins are essential for the metabolic programming of effector T cells and adaptive immunity. *Nature immunology* 14, 489–99 (2013).
8. Janowski BA, Willy PJ, Devi TR, Falck JR & Mangelsdorf DJ. An oxysterol signalling pathway mediated by the nuclear receptor LXR alpha. *Nature* 728–731 (1996).
9. Phillips, M. C. Molecular Mechanisms of Cellular Cholesterol Efflux. *Journal of Biological Chemistry* 289, 24020–24029 (2014).
10. Armstrong, A. J., Gebre, A. K., Parks, J. S. & Hedrick, C. C. ATP-Binding Cassette Transporter G1 Negatively Regulates Thymocyte and Peripheral Lymphocyte Proliferation. *The Journal of Immunology* 184, 173–183 (2010).
11. Cheng, H.-Y. *et al.* Loss of ABCG1 influences regulatory T cell differentiation and atherosclerosis. *Journal of Clinical Investigation* (2016). doi:10.1172/JCI83136
12. Hansson, G. K., Holm, J. & Jonasson, L. Detection of Activated T Lymphocytes in the Human Atherosclerotic Plaque. 7
13. Frostegård, J. *et al.* Cytokine expression in advanced human atherosclerotic plaques: dominance of pro-inflammatory (Th1) and macrophage-stimulating cytokines. *Atherosclerosis* 145, 33–43 (1999).
14. Zhou, X., Paulsson, G., Stemme, S. & Hansson, G. K. Hypercholesterolemia is associated with a T helper (Th) 1/Th2 switch of the autoimmune response in atherosclerotic apo E-knockout mice. *Journal of Clinical Investigation* 101, 1717–1725 (1998).
15. Voloshyna, I., Littlefield, M. J. & Reiss, A. B. Atherosclerosis and interferon-γ: New insights and therapeutic targets. *Trends in Cardiovascular Medicine* 24, 45–51 (2014).
16. Foks, A. C., Lichtman, A. H. & Kuiper, J. Treating atherosclerosis with regulatory T cells. *Arteriosclerosis, thrombosis, and vascular biology* 35, 280–287 (2015).
17. Howe, V. *et al.* Cholesterol homeostasis: How do cells sense sterol excess? *Chemistry and Physics of Lipids* 199, 170–178 (2016).
18. Lange, Y. & Steck, T. L. Active membrane cholesterol as a physiological effector. *Chemistry and Physics of Lipids* 199, 74–93 (2016).
19. Fessler, M. B. Regulation of Adaptive Immunity in Health and Disease by Cholesterol Metabolism. *Current Allergy and Asthma Reports* 15, (2015).
20. Yang, W. *et al.* Potentiating the antitumour response of CD8+ T cells by modulating cholesterol metabolism. *Nature* 531, 651–655 (2016).

21. Surls, J. *et al.* Increased Membrane Cholesterol in Lymphocytes Diverts T-Cells toward an Inflammatory Response. *PLoS ONE* 7, e38733 (2012).
22. Pollock, A. H. *et al.* Prolonged Intake of Dietary Lipids Alters Membrane Structure and T Cell Responses in LDLr $^{-/-}$ Mice. *The Journal of Immunology* 196, 3993–4002 (2016).
23. Dubland, J. A. & Francis, G. A. Lysosomal acid lipase: at the crossroads of normal and atherogenic cholesterol metabolism. *Frontiers in Cell and Developmental Biology* 3, (2015).
24. Zechner, R., Madeo, F. & Kratky, D. Cytosolic lipolysis and lipophagy: two sides of the same coin. *Nature Reviews Molecular Cell Biology* 18, 671–684 (2017).
25. Ouimet, M. *et al.* Autophagy Regulates Cholesterol Efflux from Macrophage Foam Cells via Lysosomal Acid Lipase. *Cell Metabolism* 13, 655–667 (2011).
26. Frodermann, V. *et al.* Heat-killed *Staphylococcus aureus* reduces atherosclerosis by inducing anti-inflammatory macrophages. *Journal of Internal Medicine* 279, 592–605 (2016).
27. Van Eck, M. *et al.* Scavenger receptor BI facilitates the metabolism of VLDL lipoproteins in vivo. *Journal of Lipid Research* 49, 136–146 (2008).
28. Schindelin, J. *et al.* Fiji: an open-source platform for biological-image analysis. *Nature Methods* 9, 676–682 (2012).
29. Du, G. *et al.* Spatial Dynamics of DNA Damage Response Protein Foci along the Ion Trajectory of High-LET Particles. *Radiation Research* 176, 706–715 (2011).
30. Kamentsky, L. *et al.* Improved structure, function and compatibility for CellProfiler: modular high-throughput image analysis software. *Bioinformatics* 27, 1179–1180 (2011).
31. Steinbrecher, U. Receptors for oxidized low density lipoprotein. *Biochimica et Biophysica Acta (BBA) - Molecular and Cell Biology of Lipids* 1436, 279–298 (1999).
32. Tan, H. *et al.* Integrative Proteomics and Phosphoproteomics Profiling Reveals Dynamic Signaling Networks and Bioenergetics Pathways Underlying T Cell Activation. *Immunity* 46, 488–503 (2017).
33. Ito, A. *et al.* Cholesterol Accumulation in CD11c+ Immune Cells Is a Causal and Targetable Factor in Autoimmune Disease. *Immunity* 45, 1311–1326 (2016).
34. Klionsky, D. J. *et al.* Guidelines for the use and interpretation of assays for monitoring autophagy. *Autophagy* 8, 445–544 (2012).
35. Tolleshaug, H. & Berg, T. Chloroquine reduces the number of asialo-glycoprotein receptors in the hepatocyte plasma membrane. *Biochemical Pharmacology* 28, 2919–2922 (1979).
36. Hubbard, V. M. *et al.* Macroautophagy regulates energy metabolism during effector T cell activation. *Journal of immunology (Baltimore, Md. : 1950)* 185, 7349–57 (2010).
37. Thiam, A. R. & Beller, M. The why, when and how of lipid droplet diversity. *Journal of Cell Science* 130, 315–324 (2017).
38. den Brok, M. H., Raaijmakers, T. K., Collado-Camps, E. & Adema, G. J. Lipid Droplets as Immune Modulators in Myeloid Cells. *Trends in Immunology* (2018). doi:10.1016/j.it.2018.01.012
39. Bozza, P. T., Magalhães, K. G. & Weller, P. F. Leukocyte lipid bodies — Biogenesis and functions in inflammation. *Biochimica et Biophysica Acta (BBA) - Molecular and Cell Biology of Lipids* 1791, 540–551 (2009).
40. Benador, I. Y. *et al.* Mitochondria Bound to Lipid Droplets Have Unique Bioenergetics, Composition, and Dynamics that Support Lipid Droplet Expansion. *Cell Metabolism* 27, 869-885.e6 (2018).
41. Kim, J., Kundu, M., Viollet, B. & Guan, K.-L. AMPK and mTOR regulate autophagy through direct phosphorylation of Ulk1. *Nature Cell Biology* 13, 132–141 (2011).
42. Hiroshi Suzuki, (...), & Tatsuhiko Kodama. A role for macrophage scavenger receptors in atherosclerosis and susceptibility to infection. 292–296 (1997).

43. Park, Y. M. CD36, a scavenger receptor implicated in atherosclerosis. *Experimental & molecular medicine* 46, e99–e99 (2014).
44. Razani, B., Feng, C. & Semenkovich, C. F. p53 is required for chloroquine-induced atheroprotection but not insulin sensitization. *The Journal of Lipid Research* 51, 1738–1746 (2010).
45. Thurnher, M. & Gruenbacher, G. T lymphocyte regulation by mevalonate metabolism. *Science Signaling* 8, re4–re4 (2015).
46. Caspar-Bauguil, S. *et al.* Mildly oxidized low-density lipoproteins suppress the proliferation of activated CD4+ T-lymphocytes and their interleukin 2 receptor expression in vitro. *Biochemical Journal* 330, 659–666 (1998).
47. Fessler, M. B. The Intracellular Cholesterol Landscape: Dynamic Integrator of the Immune Response. *Trends in Immunology* 37, 819–830 (2016).
48. Molnár, E. *et al.* Cholesterol and Sphingomyelin Drive Ligand-independent T-cell Antigen Receptor Nanoclustering. *Journal of Biological Chemistry* 287, 42664–42674 (2012).
49. Swamy, M. *et al.* A Cholesterol-Based Allostery Model of T Cell Receptor Phosphorylation. *Immunity* 44, 1091–1101 (2016).
50. Herold, M. *et al.* Liver X receptor activation promotes differentiation of regulatory T cells. *PLOS ONE* 12, e0184985 (2017).
51. Svensson, S. Crystal structure of the heterodimeric complex of LXR and RXR ligand-binding domains in a fully agonistic conformation. *The EMBO Journal* 22, 4625–4633 (2003).
52. Takeuchi, H. *et al.* Retinoid X Receptor Agonists Modulate Foxp3+ Regulatory T Cell and Th17 Cell Differentiation with Differential Dependence on Retinoic Acid Receptor Activation. *The Journal of Immunology* 191, 3725–3733 (2013).
53. Walcher, D. LXR Activation Reduces Proinflammatory Cytokine Expression in Human CD4-Positive Lymphocytes. *Arteriosclerosis, Thrombosis, and Vascular Biology* 26, 1022–1028 (2006).
54. Fantini, M. C., Dominitzki, S., Rizzo, A., Neurath, M. F. & Becker, C. In vitro generation of CD4+CD25+ regulatory cells from murine naive T cells. *Nature Protocols* 2, 1789–1794 (2007).
55. De Rosa, V. *et al.* Glycolysis controls the induction of human regulatory T cells by modulating the expression of FOXP3 exon 2 splicing variants. *Nature Immunology* (2015). doi:10.1038/ni.3269
56. Bowden, K. L. *et al.* Lysosomal Acid Lipase Deficiency Impairs Regulation of *ABCA1* Gene and Formation of High Density Lipoproteins in Cholesteryl Ester Storage Disease. *Journal of Biological Chemistry* 286, 30624–30635 (2011).
57. Thome, R. *et al.* Chloroquine-treated dendritic cells require STAT1 signaling for their tolerogenic activity. *European Journal of Immunology* 48, 1228–1234 (2018).
58. Thomé, R. *et al.* Chloroquine Treatment Enhances Regulatory T Cells and Reduces the Severity of Experimental Autoimmune Encephalomyelitis. *PLoS ONE* 8, e65913 (2013).
59. Raker, V. K., Domogalla, M. P. & Steinbrink, K. Tolerogenic Dendritic Cells for Regulatory T Cell Induction in Man. *Frontiers in Immunology* 6, (2015).
60. Huang, L.-Y., Ishii, K. J., Akira, S., Aliberti, J. & Golding, B. Th1-Like Cytokine Induction by Heat-Killed Brucella abortus Is Dependent on Triggering of TLR9. *The Journal of Immunology* 175, 3964–3970 (2005).
61. Oh, S. *et al.* Anti-inflammatory activity of chloroquine and amodiaquine through p21-mediated suppression of T cell proliferation and Th1 cell differentiation. *Biochemical and Biophysical Research Communications* 474, 345–350 (2016).
62. Pua, H. H., Dzhagalov, I., Chuck, M., Mizushima, N. & He, Y.-W. A critical role for the autophagy gene Atg5 in T cell survival and proliferation. *The Journal of Experimental Medicine* 204, 25–31 (2007).

63. Shen, K.-Y. *et al.* Molecular Mechanisms of TLR2-Mediated Antigen Cross-Presentation in Dendritic Cells. *The Journal of Immunology* 192, 4233–4241 (2014).
64. Bozzacco, L. *et al.* Strategy for Identifying Dendritic Cell-Processed CD4+ T Cell Epitopes from the HIV Gag p24 Protein. *PLoS ONE* 7, e41897 (2012).
65. Bhattacharya, A., Parillon, X., Zeng, S., Han, S. & Eissa, N. T. Deficiency of Autophagy in Dendritic Cells Protects against Experimental Autoimmune Encephalomyelitis. *Journal of Biological Chemistry* 289, 26525–26532 (2014).
66. Accapezzato, D. *et al.* Chloroquine enhances human $CD8^+$ T cell responses against soluble antigens in vivo. *The Journal of Experimental Medicine* 202, 817–828 (2005).

SUPPLEMENTARY TABLES

Table 1 Antibodies/dyes used for flow cytometry

antigen	label	clone	manufacturer
CD25	FITC	PC61.5	eBioscience
CD4	PE	GK1.5	eBioscience
CD4	eFluor 405	GK1.5	eBioscience
CD4	PerCP	RM4-5	BD Biosciences
CD44	eFluor 405	IM7	eBioscience
CD44	PE-Cy7	IM7	eBioscience
CD62L	PerCP-Cy5.5	MEL-14	eBioscience
T-bet	Alexe Fluor 647	4B10	eBioscience
FoxP3	eFluor 405	FJK-16s	eBioscience
FoxP3	APC	FJK-16s	eBioscience
Ki-67	FITC	SolA15	eBioscience
IL-2	APC	JES6-5H4	Biolegend
IL-2	APC	JES6-5H4	eBioscience
Thy1.2	PE-Cy7	53-2.1	eBioscience
eFluor 780 viability dye	APC-Cy7	-	eBioscience

Table 2 List of primers used for qRT-PCR

Gene	Forward primer (5′-3′)	Reverse primer (3′-5′)
Abca1	agagcaaaaagcgactccacatagaa	cggccacatccacaactgtct
Abcg1	ttgacaccatcccagcctac	cagtgcaggtcttctcggt
Plin2	gcacagtgccaaccagaaaattcagg	cagtctggcatgtagtctggagctg
CD36	atggtagagatggccttacttggg	agatgtagccagtgtatatgtaggctc
Rpl27	cgccaagcgatccaagatcaagtcc	agctgggtccctgaacacatccttg
Rpl37	agagacgaaacactaccgggactgg	cttgggtttcggcgttgttccctc
36B4	ctgagtacaccttcccacttactga	cgactcttcctttgcttcagcttt